Statistical evaluation of flutter boundaries from flight flutter test data

A. A. Abbasi
School of Mechanical, Aerospace and Civil Engineering,
University of Manchester
Manchester UK

J. E. Cooper
Department of Engineering,
University of Liverpool,
Liverpool, UK

ABSTRACT

A methodology is described that determines the statistical confidence bounds on the results from flight flutter tests: modal parameter estimates, flutter margin values and flutter speed estimates, without the need for Monte-Carlo simulation. The approach is based on least squares statistics and eigenvalue perturbation theory applied to the various stages of the analysis process, starting with frequency and damping estimation through to the flutter margin calculations. The technique is demonstrated upon a number of data sets from aeroelastic simulations of flight flutter tests.

NOMENCLATURE

a_i	difference equation coefficients
A,A_B	sparse Hessenberg matrix of θ and B_i terms
b_i	coefficients of flutter margin characteristic polynomial
B_i	coefficients of flutter prediction equation
B_{iU} B_{iL}	upper/lower confidence bound on B_i coefficients
d	perturbation value for a parameter
dt	time interval (s)
E	expected value
$\underline{f}$	vector of flutter margin values
F	flutter margin value
F_U, F_L	upper and lower confidence bound on flutter margin value
$\underline{J}$	vector of parameter perturbation terms
J	matrix of all parameter perturbation terms
$_k$	kth value of a parameter
m	total number of sensors
M	number of modes for the model
nf	total number of test points
N, N_B	perturbation matrix of a_i parameters, B_i terms
NO	total number of data measurements
$_0$	unperturbed value of a parameter
V	airspeed (ms^{-1})
V_F	flutter speed (ms^{-1})
V_U, V_L	upper and lower confidence bound on flutter speed (ms^{-1})
$\underline{x}_{Rk}$, $\underline{x}_{VRk}$	right eigenvector corresponding to kth term of μ, μ_v
$\underline{x}_{Lk}$, $\underline{x}_{VLk}$	left eigenvector corresponding to kth term of μ, μ_v
$x_{Rs,k}$, $x_{VRq,k}$	sth/qth element of right eigenvector corresponding to kth term of μ, μ_v
$x_{Lk,r}$, $x_{VLk,p}$	rth/pth element of left eigenvector corresponding to kth term of μ, μ_v
X_R, X_{VR}, X_L, X_{VL}	right and left eigenvectors matrix of μ, μ_v

Paper No. 3203. Manuscript received 6 June 2007, accepted 27 March 2008.

https://doi.org/10.1017/S0001924000002761 Published online by Cambridge University Press

$\underline{y}_n$	decay response data from all sensors at time instant n
$\underline{Y}$	response data vector
α, β	real and imaginary part of the eigenvalue of system modal parameters
Δ, Δ_B	matrix of unity second norm
$\underline{e}_n$	residuals error from all sensors at time instant n
$\underline{e}$/ $\underline{e}_F$	vector of residuals in response data/flutter margin values
ζ	damping ratio
$\underline{h}$, $\underline{h}_B$	perturbation terms vector of a_i parameters, B_i terms
$\underline{q}$, $\underline{q}_B$	vector of a_i parameters, B_i terms
λ	eigenvalues of system modal parameters (system eigenvalues)
μ	roots of modal parameters characteristic polynomial (eigenvalues)
μ_v	roots of flutter prediction equation (flutter speed eigenvalues)
Σ	expected value of noise
ϕ, ϕ_V	matrix of response data, airspeeds
ω	natural frequency (rad/s)

1.0 INTRODUCTION

Flutter is a destructive unstable vibration that can lead to structural failure[1-3], and it must be avoided in aircraft designs. Although the first recorded flutter incident was the Handley Page 0/400 bomber in 1916, the history of flight flutter testing began in the mid 1930s when Von Schlippe conducted the first ever recorded tests to measure the amplitude of the structural response to the excitation so as to determine the safe flight conditions. Since then, flight flutter testing[4,5] has matured to become a critical stage in the certification process providing the final validation of the analytical predictions.

Flight flutter testing is undertaken to demonstrate that prototype aircraft are free of flutter throughout the desired flight envelope and also for a safety margin of typically 15-20%. The test procedure at each flight test point consists of three separate stages:

(a) The aircraft is excited in some manner (e.g. using the flight control system, aerodynamic vanes or inertia exciters) and the response measured, typically with accelerometers attached to various parts of the structure
(b) The excitation and response data sets are curve-fitted using some form of system identification algorithm from which the frequencies, damping ratios and sometimes mode shapes are estimated.
(c) The decision is made as whether it is safe to proceed to the next flight test point.

The most critical stage is the final one as, at this point, test engineers are required to decide whether the flight envelope can be expanded further and whether it is safe to move on to the next test point. This is usually achieved by determining the flutter speed using the measured test data, and also comparison with the aircraft aeroelastic model. There are a number of different ways that the flutter speed can be predicted, either by using the identified modal parameters or the estimated mathematical model of the aeroelastic system.

Damping extrapolation[4] is the most commonly used approach even though there can be concerns over its accuracy, as damping is the most sensitive parameter to identify and the onset of instabilities with airspeed increase may be very sudden. A second technique, the flutter margin method[6], is also often used and is based on the Routh-Hurwitz stability criterion to predict the flutter onset speed assuming a binary flutter mechanism. There are a range of other possible approaches. The Nissim-Gilyard method[7] identifies the aeroelastic equations of motion which can then be used to predict the flutter speed at different flight conditions. An alternative approach is the envelope function[8,9], which does not require modal parameter estimates but defines the trend of the overall stability of the impulse response time envelope boundary with varying flight condition. The discrete-time ARMA model approach[10] is based on random excitation time histories and provides results similar to those of flutter margin method. Several of these methods have been compared using simulated[11] and flight test[12] data.

A recent advance in the flutter prediction process has been to introduce statistical approaches for the prediction of flutter boundaries. The Flutterometer[13,14] is a technique which can be used to determine robust flutter margins[15,16] of an aeroelastic model. Once the first flight test point results are estimated, the difference between the corresponding parameters provides a measure for the uncertainty in the model. Then μ-analysis results provide the lowest flutter speed for the worst combination of uncertainty parameters. This technique can feasibly be used to clear the flight envelope by testing a single point only[17].

The issue related to the modal parameter estimates confidence bounds or their sensitivity to the noise in response has been addressed in different ways using both time domain and frequency domain approaches, either using Monte Carlo simulations[18-22] or perturbation analysis[23-26]. As seen in a number of studies[5,21,27,28], both the frequency and damping ratio estimates are normally distributed if the noise statistics are also Gaussian zero mean.

However, little evaluation of the propagation of uncertainty in modal parameters and their effect on the resulting flutter speed prediction has been made. In recent years, work by Poirel *et al*[27] has considered the statistics of the flutter margin method via an approach based upon Monte-Carlo simulations or results from multiple tests at the same condition. Their findings were extended by another study at NASA[29] that investigated results for flutter speed prediction using historical wind tunnel experimental data sets where repeated flutter tests were conducted on different occasions.

In this paper, a more rigorous approach towards calculating the statistics for the flutter margin is demonstrated. Initially, the statistics on frequency and damping ratio estimates from least squares based time domain identification algorithms are determined and then extended to apply to the flutter speed predictions from the flutter margin method[6]. This statistical approach enables the flutter speed bounds to be determined by considering the estimates from each flight test point without the need for Monte-Carlo simulations and repetition of test under the same flight conditions. The methodology is validated using several simulated aeroelastic test cases and the results are compared with Monte-Carlo simulations.

2.0 UNDERLYING PROCEDURE

2.1 Modal parameter estimation

Most time domain system identification methods employ the least squares solution[30] as their fundamental component, e.g. the least squares complex exponential (LSCE) method[31] and its multiple input-multiple output extension, polyreference[32]. The eigensystem realisation algorithm[33] and most sub-space methods[34] develop minimum realisation solutions again with least squares as a major part of their formulation. In this work, the modal parameter estimation is based on the LSCE method.

The decay response model can be written in difference equation form as

$$\underline{y}_i + a_1 \underline{y}_{i-1} + a_2 \underline{y}_{i-2} + \cdots + a_{2M} \underline{y}_{i-2M} = \underline{\varepsilon}_i \qquad \ldots (1)$$

where $\underline{y}_i$ is the output response vector ($m \times 1$) from all the measurement stations at time instant i, the a_i parameters represent the coefficients of the difference equation model and $\underline{e}_i$ represents the residual noise containing corruption from all measurement stations.

https://doi.org/10.1017/S0001924000002761 Published online by Cambridge University Press

In compact form, Equation (1) becomes

$$\underline{Y} = \phi\underline{\theta} + \underline{\varepsilon} \quad \ldots (2)$$

where $\boldsymbol{\phi}$ is the data matrix and $\underline{\theta}$ comprises the unknown a_i parameters, the least squares solution is

$$\underline{\theta} = \left(\phi^T\phi\right)^{-1}\phi^T\underline{Y} \quad \ldots (3)$$

The frequencies and dampings are found from the roots of the characteristic polynomial

$$\mu^{2M} + a_1\mu^{2M-1} + \cdots + a_{2M-1}\mu + a_{2M} = 0 \quad \ldots (4)$$

where M denotes the number of modes and the kth mode roots take the form

$$\mu_k = \exp\left(\left[-\zeta_k\omega_k \pm j\omega_k\sqrt{1-\zeta_k^2}\right]dt\right) = \exp\left(\left(\alpha_k \pm j\beta_k\right)dt\right) = \exp\left(\lambda_k dt\right) \quad \ldots (5)$$

and the frequencies ω_k and damping ratios ζ_k are found as

$$\omega_k = \left|\lambda_k\right| \quad \text{and} \quad \zeta_k = -\frac{\alpha_k}{\omega_k} \quad \ldots (6)$$

Due to the least squares element of the algorithm, LSCE estimates are biased in the presence of noise (as is the case in flutter testing)[30] and thus overspecified mathematical models must be used in order to reduce the bias. Techniques such as stability plots then have to be applied in order to distinguish system from spurious modes.

2.2 Flutter margin method

At each flight test point, the identified frequencies and damping ratios of the two modes that combine to cause flutter are considered. The two pairs of complex conjugate roots

$$\lambda_{1,2} = \alpha_1 \pm j\beta_1 \quad \text{and} \quad \lambda_{3,4} = \alpha_2 \pm j\beta_2 \quad \ldots (7)$$

can be combined to form the characteristic equation

$$b_4\lambda^4 + b_3\lambda^3 + b_2\lambda^2 + b_1\lambda + b_0 = 0 \quad \ldots (8)$$

where

$$\begin{aligned} &b_4 = 1; \quad b_3 = -2\left(\alpha_1 + \alpha_2\right); \\ &b_2 = {\alpha_1}^2 + {\alpha_2}^2 + 4\alpha_1\alpha_2 + \beta_1^2 + \beta_2^2 \\ &b_1 = -2\left(\alpha_1{\alpha_2}^2 + \alpha_1\beta_2^2 + \alpha_2{\alpha_1}^2 + \alpha_2\beta_1^2\right); \\ &b_0 = {\alpha_1}^2{\alpha_2}^2 + {\alpha_1}^2\beta_2^2 + {\alpha_2}^2\beta_1^2 + \beta_1^2\beta_2^2 \end{aligned} \quad \ldots (9)$$

The flutter margin method[6] determines the remaining Routh-Hurwitz stability by applying the expression

$$b_2\left(\frac{b_1}{b_3}\right) - \left(\frac{b_1}{b_3}\right)^2 - b_0 > 0 \quad \Rightarrow \quad \left(\left(\frac{b_2}{2}\right)^2 - b_0\right) - \left(\frac{b_2}{2} - \frac{b_1}{b_3}\right)^2 > 0 \quad \ldots (10)$$

and the flutter margin (F) is usually defined from Equation (10) as

$$\begin{aligned} F &= \left[\left(\frac{b_2}{2}\right)^2 - b_0\right] - \left(\frac{b_2}{2} - \frac{b_1}{b_3}\right)^2 \\ &= \left[\left(\frac{\beta_2^2}{2} - \frac{\beta_1^2}{2}\right) + \left(\frac{\alpha_2^2}{2} - \frac{\alpha_1^2}{2}\right)\right]^2 \\ &+ 4\alpha_1\alpha_2\left[\left(\frac{\beta_2^2 + \beta_1^2}{2}\right) + 2\left(\frac{\alpha_2 + \alpha_1}{2}\right)^2\right] \\ &- \left[\left(\frac{\alpha_2 - \alpha_1}{\alpha_2 + \alpha_1}\right)\left(\frac{\beta_2^2 - \beta_1^2}{2}\right) + 2\left(\frac{\alpha_2 + \alpha_1}{2}\right)^2\right]^2 \end{aligned} \quad \ldots (11)$$

Flutter margins are calculated at a number of dynamic pressures and a quadratic curve fitted in the form

$$F = B_2q^2 + B_1q + B_0 \quad \ldots (12)$$

in order to determine the unknown B_i values. The curve is extrapolated and the flutter speed V_F (or dynamic pressure) is determined when $F = 0$. An alternative way to predict the flutter speed is to find the eigenvalues of sparse Hessenberg matrix $\mathbf{A_B}$ where

$$\mathbf{A_B} = \begin{bmatrix} 0 & -B_0/B_2 \\ 1 & -B_1/B_2 \end{bmatrix} \quad \ldots (13)$$

Although the flutter prediction Equation (12) is often written in terms of the dynamic pressure q, it can also be applied in terms of the equivalent airspeed V without compromising the quadratic form of the flutter prediction curve, but with the assumption that the flight altitude remains constant. Numerous examples of this approach to indicate flutter onset are found in previous studies, including the original Zimmerman work[6,11,35,36]. Here, further statistical analysis of the flutter prediction process will be carried out in terms of airspeed V.

3.0 STATISTICAL APPROACH

The underlying procedure is extended to determine the statistical bounds at each of the steps required to determine the flutter speed. The errors in each part feed into the final flutter speed calculation.

3.1 Statistics on the difference equation parameters and corresponding eigenvalues

Combining Equations (2) and (3) gives

$$\underline{\theta} = \underline{\theta}_{Truth} + \left(\phi^T\phi\right)^{-1}\phi^T\underline{\varepsilon} \quad \ldots (14)$$

where the form of the error on the least squares solution can be seen. The covariance matrix $\mathbf{D_0}$, whose diagonal values are the variances of a_i parameters, is defined as

$$\begin{aligned} D_\theta &= \left(\underline{\theta} - \underline{\theta}_{truth}\right)\left(\underline{\theta} - \underline{\theta}_{truth}\right)^T = \left(\phi^T\phi\right)^{-1}\phi^T\underline{\varepsilon}\underline{\varepsilon}^T\phi\left(\phi^T\phi\right)^{-1} \\ &= \left(\phi^T\phi\right)^{-1}\phi^T\Sigma\phi\left(\phi^T\phi\right)^{-1} \end{aligned} \quad \ldots (15)$$

where $\Sigma = E(\underline{\varepsilon}\underline{\varepsilon}^T)$, is the expected value of the residual term.

The assumption of Gaussian distributed uncorrelated noise data has been made in numerous studies[8,19,21,23,29,37-43] and the expected value becomes

$$\Sigma = E\left(\underline{\varepsilon}\underline{\varepsilon}^T\right) = \sigma_\varepsilon^2 I \quad \ldots (16)$$

where σ_ε^2 represents the variance of the noise signal, thus

$$D_\theta = \left(\phi^T\phi\right)^{-1}\sigma_\varepsilon^2 I \quad \ldots (17)$$

Hence, the variance σ_q^2 on each element of $\underline{q}$ can be identified from the corresponding diagonal values of D_q.

The next step is to find the effect of noise on the eigenvalues of the system[37]. The eigenvalues of the sparse Hessenburg matrix

$$\mathbf{A} = \underset{(2M\times 2M)}{\begin{bmatrix} 0 & 0 & \cdots & -a_{2M} \\ 1 & 0 & \cdots & -a_{2M-1} \\ \vdots & \vdots & \ddots & \vdots \\ 0 & 0 & 1 & -a_1 \end{bmatrix}} \quad \ldots (18)$$

https://doi.org/10.1017/S0001924000002761 Published online by Cambridge University Press

are the same as the roots of Equation (4) and take the form as shown in Equation (5). For an underdamped system, matrix **A** has the classical eigenvalue solution for corresponding right (classical) eigenvectors $\underline{x}_{R_k}$ and left eigenvectors $\underline{x}_{L_k}$[44] such that

$$\left(\mathbf{A}-\mu_k I\right)\underline{x}_{R_k}=0 \quad \text{and} \quad \left(\mathbf{A}^T-\mu_k I\right)\underline{x}_{L_k}^T=0 \qquad \ldots (19)$$

Considering that matrix **A** is subjected to a small perturbation, $N = \Delta\eta$, (where η is scalar quantity and Δ is such that $\|\Delta\|_2 = 1$) and using function theory[44], Equation (19) is modified to show the changes in the eigenvalues μ_k and eigenvectors $\underline{x}_{R_k}$ as functions of η

$$\left(\mathbf{A}+\Delta\eta\right)\underline{x}_{R_k}(\eta)=\mu_k(\eta)\,\underline{x}_{R_k}(\eta) \qquad \ldots (20)$$

and then differentiated with respect to η around the origin and setting $\eta = 0$ and $\mu_k(0) = \mu_k$ and $\underline{x}_{R_k}(0) = \underline{x}_{R_k}$ leads to

$$\begin{aligned}&\mathbf{A}\frac{\mathrm{d}}{\mathrm{d}\eta}\left(\underline{x}_{R_k}\right)+\Delta\underline{x}_{R_k}\frac{\mathrm{d}}{\mathrm{d}\eta}(\eta)+\Delta\eta\frac{\mathrm{d}}{\mathrm{d}\eta}\left(\underline{x}_{R_k}\right)\\&=\frac{\mathrm{d}}{\mathrm{d}\eta}(\mu_k)\,\underline{x}_{R_k}+\mu_k\frac{\mathrm{d}}{\mathrm{d}\eta}\left(\underline{x}_{R_k}\right) \quad\Rightarrow\quad \Delta\underline{x}_{R_k}=\frac{\mathrm{d}}{\mathrm{d}\eta}(\mu_k)\,\underline{x}_{R_k}\end{aligned} \qquad \ldots (21)$$

Pre-multiplying both sides with $\underline{x}_{L_k}^H$ and taking the absolutes, the Equation (21) leads to

$$\mathrm{d}\mu_k=\frac{\underline{x}_{L_k}^H\Delta\underline{x}_{R_k}}{\underline{x}_{L_k}^H\underline{x}_{R_k}} \qquad \ldots (22)$$

Therefore, sensitivity of the kth eigenvalue due to a small perturbation $N = \Delta\eta$ can be shown in terms of its corresponding left and right eigenvectors. If the perturbation on each element of matrix **A** is represented by the term η_{rs} of the matrix **N** (same order as **A**) given by,

$$\mathbf{N}=\begin{bmatrix}0&0&\cdots&\eta_{1,2M}\\0&0&\cdots&\eta_{2,2M}\\\vdots&\vdots&\ddots&\vdots\\0&0&\cdots&\eta_{2M,2M}\end{bmatrix} \qquad \ldots (23)$$

then by chain rule expansion on the resulting perturbation terms in μ_k, and considering the summations of individual perturbation terms, it can be found that

$$\begin{aligned}&\mathrm{d}\mu_k=\sum_{rs}\left(\frac{\partial\mu_k}{\partial\eta_{rs}}\right)\mathrm{d}\eta_{rs};\quad \frac{\partial\mu_k}{\partial\eta_{rs}}=\frac{\underline{x}_{L_{k,r}}^H\underline{x}_{R_{s,k}}}{\underline{x}_{L_k}^H\underline{x}_{R_k}}\\&\Rightarrow \mathrm{d}\mu_k=\sum_{rs}\frac{\underline{x}_{L_{k,r}}^H\underline{x}_{R_{s,k}}}{\underline{x}_{L_k}^H\underline{x}_{R_k}}\eta_{rs}=\underline{J}_{\mu_k}^T\underline{\eta}\end{aligned} \qquad \ldots (24)$$

where $\underline{x}_{L_{k,r}}$ and $\underline{x}_{R_{s,k}}$ are the rth and sth elements of the kth left and right eigenvector, respectively, representing their $2M$th term as does the perturbation vector $\underline{\boldsymbol{\eta}}$, taken from the perturbation matrix **N**, and hence the vector of the kth eigenvalue perturbation terms is of the order $(2M \times 1)$.

Expanding the above expression using a Maclaurin series expansion up to first order terms yields

$$\begin{aligned}&\mu_k(\eta)=\mu_k(\eta=0)+\mathrm{d}\mu_k(\eta)(\eta-\eta_0)\\&=\mu_{k_0}+\mathrm{d}\mu_k(\eta)=\mu_{k_0}+\underline{J}_{\mu_k}^T\underline{\eta}\end{aligned} \qquad \ldots (25)$$

and keeping all the perturbed eigenvalues in vector form it can be shown that

$$\underline{\mu}-\underline{\mu}_0=\mathbf{J}_\mu\underline{\eta} \quad \text{and} \quad \left(\underline{\mu}-\underline{\mu}_0\right)^H=\underline{\eta}^T J_\mu^H \qquad \ldots (26)$$

where $\mathbf{J}_\mu$ is the matrix of perturbation terms of the corresponding eigenvalues. If $\underline{h}$ is known then the perturbed eigenvalues $\underline{m}$ can be found and the covariance matrix $\boldsymbol{D}_\mu$ for the eigenvalues becomes

$$\mathbf{D}_\mu=E\left(J_\mu\underline{\eta}\underline{\eta}^T J_\mu^H\right)=J_\mu E\left(\underline{\eta}\underline{\eta}^T\right)J_\mu^H \qquad \ldots (27)$$

As $\underline{\boldsymbol{\eta}}$ is the vector of error terms found by calculating the variances of a_i parameters and its expected value $E(\underline{h}\underline{h}^T)$ can be taken as D_η, therefore the diagonal values of the matrix $\mathbf{D}_\mu$ are the variances σ_m^2 on the eigenvalues and including the covariance matrix definition from Equation (17) gives

$$\begin{aligned}&\mathbf{D}_\mu=J_\mu D_\theta J_\mu^H \quad\Rightarrow \sigma_\mu{}^2=\mathrm{diag}\left(J_\mu D_\theta J_\mu^H\right)\\&\&\quad \sigma_\mu{}^2/\sigma_\varepsilon^2=\mathrm{diag}\left(J_\mu\left(\phi^T\phi\right)^{-1}J_\mu^H\right)\end{aligned} \qquad \ldots (28)$$

The diagonal terms of the matrix in Equation (28) represent the sensitivity of each eigenvalue and, hence, each mode due to noise in the data. Therefore, it is possible to determine which of the eigenvalues has the lowest variance and hence the modes with the lowest variances on the modal parameters can be identified as described in the following section. It would be feasible to measure the response before testing commences at each flight condition in order to establish the statistics of the noise, however, the assumption is then made that the same noise behaviour is experienced during the test.

The above approach is just as applicable if SIMO or MIMO data is considered. There is no need for averaging of results from different transducers or generation of pseudo data sets based upon a pre-supposed statistical distribution.

One difficulty is that overspecification of the model order is required when using time domain system identification methods in order to produce unbiased modal parameter estimates, and this results in the matrix becoming rank deficient (or near rank deficient) resulting in numerical problems occurring with the inverse calculation in Equation (28). To circumvent this problem, the singular value decomposition (SVD) was applied to the $\boldsymbol{\phi}$ matrix and only those matrix terms relating to the non (near) zero singular values were retained. The SVD approach was used throughout the rest of this work.

3.2 Statistics on the system eigenvalues

The eigenvalues of the system[41] are given by

$$\lambda_k=\ln(\mu_k)/\mathrm{d}t \quad\Rightarrow\quad \lambda_k(\eta)=\ln(\mu_k(\eta))/\mathrm{d}t \qquad \ldots (29)$$

thus, applying a Maclaurin series expansion and ignoring second order and higher terms and then with logarithmic series distribution to that expression and keeping only first order terms gives

$$\begin{aligned}&\lambda_k(0)+\eta\mathrm{d}\lambda_k=\frac{1}{\mathrm{d}t}\ln\left(\mu_k(0)+\eta\mathrm{d}\mu_k\right)\\&=\frac{1}{\mathrm{d}t}\ln\left(\mu_k(0)\right)+\frac{1}{\mathrm{d}t}\ln\left(1+\eta\frac{\mathrm{d}\mu_k}{\mu_k(0)}\right)\end{aligned} \qquad \ldots (30)$$

$$\begin{aligned}&\Rightarrow \eta\mathrm{d}\lambda_k=\frac{1}{\mathrm{d}t}\eta\left(\frac{\mathrm{d}\mu_k}{\mu_k}\right) \quad\Rightarrow\quad \mathrm{d}\lambda_k=\frac{1}{\mathrm{d}t}\left(\frac{\mathrm{d}\mu_k}{\mu_k}\right)\\&=\mathrm{d}\alpha_k\pm j\mathrm{d}\beta_k=\frac{1}{\mathrm{d}t}\frac{\underline{J}_{\mu_k}^T}{\mu_k}\underline{\eta}=\underline{\mathbf{J}}_{\lambda_k}^{\mathrm{T}}\underline{\eta}\end{aligned} \qquad \ldots (31)$$

where $\underline{\mathbf{J}}_{\boldsymbol{\lambda k}}$ represents the vector of the kth system eigenvalue perturbation terms. Re-writing Equation (31) for all the system eigenvalues leads to

$$\underline{\lambda}-\underline{\lambda}_0=J_\lambda\underline{\eta} \quad \text{and} \quad \left(\underline{\lambda}-\underline{\lambda}_0\right)^H=\underline{\eta}^T J_\lambda^H \qquad \ldots (32)$$

https://doi.org/10.1017/S0001924000002761 Published online by Cambridge University Press

where $\boldsymbol{J_\lambda}$ is the perturbation matrix of the system eigenvalues. Thus the variance of the system eigenvalues $\sigma_{\lambda i}^2$ are found to be as the diagonal terms of the matrix given by

$$D_\lambda = E\left(J_\lambda \underline{\eta}\underline{\eta}^T J_\lambda^H\right) = J_\lambda E\left(\underline{\eta}\underline{\eta}^T\right) J_\lambda^H \quad \ldots (33)$$

$$\sigma_\lambda{}^2 = \mathrm{diag}\left(J_\lambda D_\theta J_\lambda^H\right) = \mathrm{diag}\left(J_\lambda \left(\phi^T\phi\right)^{-1} \sigma_\varepsilon^2 J_\lambda^H\right)$$
$$\text{and} \quad \sigma_\lambda{}^2/\sigma_\varepsilon^2 = \mathrm{diag}\left(J_\lambda \left(\phi^T\phi\right)^{-1} J_\lambda^H\right) \quad \ldots (34)$$

The perturbation terms of the real and imaginary parts of these eigenvalues $d\alpha_k$ and $d\beta_k$ are

$$\mathrm{d}\alpha_k = \mathrm{Re}\left(\underline{J}_{\lambda k}^T\right)\underline{\eta} = \underline{J}_{\alpha_k}^T\underline{\eta} \quad \text{and} \quad \mathrm{d}\beta_k = \mathrm{Im}\left(\underline{J}_{\lambda k}^T\right)\underline{\eta} = \underline{J}_{\beta_k}^T\underline{\eta} \quad \ldots (35)$$

where $\underline{J}_a^T$ and $\underline{J}_b^T$ represent the perturbation vectors of the real and imaginary parts of all the system eigenvalues. Thus, if only the two modes contributing to the flutter mechanism are considered then

$$\underline{\mathrm{d}\alpha\beta} = \begin{pmatrix}\underline{\mathrm{d}\alpha}\\ \underline{\mathrm{d}\beta}\end{pmatrix} = \begin{pmatrix}\mathrm{d}\alpha_1\\ \mathrm{d}\alpha_2\\ \mathrm{d}\beta_1\\ \mathrm{d}\beta_2\end{pmatrix} = \begin{pmatrix}\underline{J}_{\alpha_1}^T\\ \underline{J}_{\alpha_2}^T\\ \underline{J}_{\beta_1}^T\\ \underline{J}_{\beta_2}^T\end{pmatrix}\underline{\eta} = \begin{pmatrix}J_\alpha^T\\ J_\beta^T\end{pmatrix}\underline{\eta} \quad \ldots (36)$$

It is possible to determine the variance on the α_k and β_k terms from the diagonal terms of relevant covariance matrices as well as the statistics of the system frequencies and damping ratios; however, these are not required in order to determine the flight condition at which flutter occurs.

3.3 Statistics on the flutter margin values

The errors in the system eigenvalues can now be introduced into the expression of the flutter margin. Small perturbations in the characteristic polynomial coefficients (Equations (9)) are given as

$$\mathrm{d}b_3 = -2\left(\mathrm{d}\alpha_1 + \mathrm{d}\alpha_2\right) \quad \ldots (37)$$

$$\mathrm{d}b_2 = 2\alpha_1\mathrm{d}\alpha_1 + 2\alpha_2\mathrm{d}\alpha_2 + 4\left(\alpha_1\mathrm{d}\alpha_2 + \alpha_2\mathrm{d}\alpha_1\right) + 2\beta_1\mathrm{d}\beta_1 + 2\beta_2\mathrm{d}\beta_2 \quad \ldots (38)$$

$$\mathrm{d}b_1 = -2\left(\begin{array}{l}\alpha_2{}^2\mathrm{d}\alpha_1 + 2\alpha_1\alpha_2\mathrm{d}\alpha_2 + \alpha_1{}^2\mathrm{d}\alpha_2 + 2\alpha_1\alpha_2\mathrm{d}\alpha_1 + \\ \beta_2^2\mathrm{d}\alpha_1 + 2\alpha_1\beta_2\mathrm{d}\beta_2 + \beta_1^2\mathrm{d}\alpha_2 + 2\alpha_2\beta_1\mathrm{d}\beta_1\end{array}\right) \quad \ldots (39)$$

$$\mathrm{d}b_0 = 2\left(\begin{array}{l}\alpha_1\alpha_2{}^2\mathrm{d}\alpha_1 + \alpha_1{}^2\alpha_2\mathrm{d}\alpha_2 + \alpha_1\beta_2{}^2\mathrm{d}\alpha_1 + \alpha_1{}^2\beta_2\mathrm{d}\beta_2 \\ +\alpha_2\beta_1{}^2\mathrm{d}\alpha_2 + \alpha_2{}^2\beta_1\mathrm{d}\beta_1 + \beta_1\beta_2{}^2\mathrm{d}\beta_1 + \beta_1{}^2\beta_2\mathrm{d}\beta_2\end{array}\right) \quad \ldots (40)$$

and Equations (37) to (40) can be combined into the form

$$\underline{\mathrm{d}b} = \begin{bmatrix}\mathrm{d}b_0\\ \mathrm{d}b_1\\ \mathrm{d}b_2\\ \mathrm{d}b_3\end{bmatrix} = J_{\alpha\beta}\begin{bmatrix}\mathrm{d}\alpha_1\\ \mathrm{d}\alpha_2\\ \mathrm{d}\beta_1\\ \mathrm{d}\beta_2\end{bmatrix} = J_{\alpha\beta}\begin{bmatrix}\underline{\mathrm{d}\alpha}\\ \underline{\mathrm{d}\beta}\end{bmatrix} = J_{\alpha\beta}\,\underline{\mathrm{d}\alpha\beta} \quad \ldots (41)$$

where

$$J_{\alpha\beta} = \begin{bmatrix} 2\left(\alpha_1\alpha_2^2 + \alpha_1\beta_2^2\right) & 2\left(\alpha_2\alpha_1^2 + \alpha_2\beta_1^2\right) & 2\left(\beta_1\alpha_2^2 + \beta_1\beta_2^2\right) & 2\left(\beta_2\alpha_1^2 + \beta_2\beta_1^2\right)\\ -2\left(\alpha_2^2 + 2\alpha_1\alpha_2 + \beta_2^2\right) & -2\left(\alpha_1^2 + 2\alpha_1\alpha_2 + \beta_1^2\right) & -4\left(\beta_1\alpha_2\right) & -4\left(\beta_2\alpha_1\right)\\ 2\left(\alpha_1 + 2\alpha_2\right) & 2\left(\alpha_2 + 2\alpha_1\right) & 2\left(\beta_1\right) & 2\left(\beta_2\right)\\ -2 & -2 & 0 & 0\end{bmatrix} \quad \ldots (42)$$

The perturbation of the flutter margin value defined in Equation (11) is given as

$$\mathrm{d}F = \left(\frac{1}{2}b_2\mathrm{d}b_2 - \mathrm{d}b_0\right) - 2\left(\frac{b_2}{2} - \frac{b_1}{b_3}\right)\left(\frac{1}{2}\mathrm{d}b_2 - \left(\frac{1}{b_3}\mathrm{d}b_1 - \frac{b_1}{b_3^2}\mathrm{d}b_3\right)\right) \quad \ldots (43)$$

which can be rewritten using Equations (36) and (41) as

$$\mathrm{d}F = \underline{J}_b^T\,\underline{\mathrm{d}b} = \underline{J}_b^T J_{\alpha\beta}\,\underline{\mathrm{d}\alpha\beta} = \underline{J}_b^T J_{\alpha\beta}\begin{pmatrix}J_\alpha^T\\ J_\beta^T\end{pmatrix}\underline{\eta} = \underline{J}_F^T\underline{\eta} \quad \ldots (44)$$

where

$$\underline{J}_b^T = \begin{bmatrix}-1 & \dfrac{b_2b_3 - 2b_1}{b_3^2} & \dfrac{b_1}{b_3} & \dfrac{2b_1^2 - b_1b_2b_3}{b_3^3}\end{bmatrix} \quad \ldots (45)$$

The variance of the flutter margin at a particular flight condition then follows as

$$\sigma_F^2 = E\left(\underline{J}_F^T\underline{\eta}\underline{\eta}^T\underline{J}_F\right) = \underline{J}_F^T E\left(\underline{\eta}\underline{\eta}^T\right)\underline{J}_F$$
$$\Rightarrow \sigma_F^2 = \underline{J}_F^T D_\theta \underline{J}_F = \underline{J}_F^T\left(\phi^T\phi\right)^{-1}\underline{J}_F\sigma_\varepsilon^2 \quad \ldots (46)$$

It should be noted that the assumption is made that the flutter margins are assumed to have a Gaussian distribution which is contrary to that found in Ref. 27. Extensive numerical simulations have shown that in most cases the distribution of the flutter margin is Gaussian (Ref. 27 is an exception). Further work is continuing to extend the methodology to deal with non-Gaussian distributions.

3.4 Statistics on the predicted flutter speed

Having determined the statistics on the flutter margins, we are interested in determining the variance of the predicted flutter speed. Two approaches will be used here.

3.4.1 Curvefitting approach

Once the statistics of the flutter margins are found, it is a simple matter to curvefit the upper and lower bounds at each flight condition as per Equation (12) and extrapolate each curve to give upper and lower flutter speed bounds.

3.4.2 Statistical approach

A more rigorous approach is to make use of the flutter margin statistics and examine the effect they have upon the flutter speed prediction of Equation (13). Considering Equation (12) for a range of different flight speeds, then the least squares solution of unknown parameters B_i is written in the form

$$\underline{\theta}_B = \left(\phi_V^T\phi_V\right)^{-1}\phi_V^T\,\underline{F} \quad \ldots (47)$$

where ϕ_v is a matrix of velocity terms and $\underline{\mathbf{F}}$ is the vector of *nf* flutter margins.

The error on the flutter margins $\underline{dF}$ propagates through to errors in the B_i terms such that

$$\underline{\theta}_B - \underline{\theta}_{B_{Truth}} = \left(\phi_V^T\phi_V\right)^{-1}\phi_V^T\left(\underline{\mathrm{d}F}\right) = \left(\phi_V^T\phi_V\right)^{-1}\phi_V^T\begin{bmatrix}\underline{J}_{F_1}^T\eta_1\\ \underline{J}_{F_2}^T\eta_2\\ \vdots\\ \underline{J}_{F_{nf}}^T\eta_{nf}\end{bmatrix} \quad \ldots (48)$$

and leads to a covariance matrix $\mathbf{D_B}$ of the B_i coefficients given by

https://doi.org/10.1017/S0001924000002761 Published online by Cambridge University Press

$$\mathbf{D}_B = \left(\phi_V^T \phi_V\right)^{-1} \phi_V^T \begin{bmatrix} \underline{J}_{F_1}^T \eta_1 \\ \underline{J}_{F_2}^T \eta_2 \\ \vdots \\ \underline{J}_{F_{nf}}^T \eta_{nf} \end{bmatrix} \begin{bmatrix} \underline{J}_{F_1}^T & \underline{\eta}_2^T \underline{J}_{F_2} & \cdots & \underline{\eta}_{nf}^T \underline{J}_{F_{nf}} \end{bmatrix} \phi_V \left(\phi_V^T \phi_V\right)^{-1} \quad \ldots (49)$$

and assuming that the noise in each flight case is independent but has the same variance, then we obtain

$$\mathbf{D}_B = \left(\phi_V^T \phi_V\right)^{-1} \begin{bmatrix} \underline{J}_{F_1}^T \mathrm{E}\left(\underline{\eta}_1 \underline{\eta}_1^T\right) \underline{J}_{F_1} & 0 & \cdots & 0 \\ 0 & \underline{J}_{F_2}^T \mathrm{E}\left(\underline{\eta}_2 \underline{\eta}_2^T\right) \underline{J}_{F_2} & \cdots & 0 \\ \vdots & \vdots & \ddots & \vdots \\ 0 & 0 & \cdots & \underline{J}_{F_{nf}}^T \mathrm{E}\left(\underline{\eta}_{nf} \underline{\eta}_{nf}^T\right) \underline{J}_{F_{nf}} \end{bmatrix} \phi_V \left(\phi_V^T \phi_V\right)^{-1} \quad \ldots (50)$$

$$\mathbf{D}_B = \left(\phi_V^T \phi_V\right)^{-1} \begin{bmatrix} \underline{J}_1^T \left(\phi^T \phi\right)_1^{-1} \underline{J}_1 & 0 & \cdots & 0 \\ 0 & \underline{J}_2^T \left(\phi^T \phi\right)_2^{-1} \underline{J}_2 & \cdots & 0 \\ \vdots & \vdots & \ddots & \vdots \\ 0 & 0 & \cdots & \underline{J}_{nf}^T \left(\phi^T \phi\right)_{nf}^{-1} \underline{J}_{nf} \end{bmatrix} \phi_V \left(\phi_V^T \phi_V\right)^{-1} \sigma_\varepsilon^2 \quad \ldots (51)$$

and hence the variance and covariance of the B_i terms can be found.

The variance of the flutter speed is found by computing the variance of the eigenvalues of matrix $\mathbf{A_B}$ in Equation (13), using the approach described in Section 3.1. One complication is that matrix $\mathbf{A_B}$ contains quotients of two random variables and we need to make use of the expressions for their variance[45-48] and covariance[49,50] values given in terms of their respective mean, variance and covariance values such that

$$\mathrm{var}(a/b) = (\bar{a}/\bar{b})^2 \left[\mathrm{var}(a)/\bar{a}^2 + \mathrm{var}(b)/\bar{b}^2 - 2\,\mathrm{cov}(a,b)/\bar{a}\bar{b} \right] \quad \ldots (52)$$

and

$$\mathrm{cov}\left(\frac{a}{b}, \frac{c}{d}\right) = \left(\frac{\bar{a}\,\bar{c}}{\bar{b}\,\bar{d}}\right)^2 \left[\frac{\mathrm{cov}(a,c)}{\bar{a}\,\bar{c}} - \frac{\mathrm{cov}(a,d)}{\bar{a}\,\bar{d}} - \frac{\mathrm{cov}(b,c)}{\bar{b}\,\bar{c}} + \frac{\mathrm{cov}(b,d)}{\bar{b}\,\bar{d}} \right] \quad \ldots (53)$$

where the functions Var and Cov represent the corresponding variance and covariance terms of the random variables a, b, c and d with their mean values as $\bar{a}$, $\bar{b}$, $\bar{c}$ and $\bar{d}$ respectively.

Hence, the corresponding variance and covariance terms become

$$\mathrm{var}\left(B_0/B_2\right) = \left(B_0/B_2\right)^2 \left[\mathrm{var}\left(B_0\right)/B_0^{\,2} + \mathrm{var}\left(B_2\right)/B_2^{\,2} - 2\,\mathrm{cov}\left(B_0, B_2\right)/B_0 B_2 \right] \quad \ldots (54)$$

$$\mathrm{var}\left(B_1/B_2\right) = \left(B_1/B_2\right)^2 \left[\mathrm{var}\left(B_1\right)/B_1^{\,2} + \mathrm{var}\left(B_2\right)/B_2^{\,2} - 2\,\mathrm{cov}\left(B_1, B_2\right)/B_1 B_2 \right] \quad \ldots (55)$$

$$\mathrm{cov}\left(\frac{B_0}{B_2}, \frac{B_1}{B_2}\right) = \left(\frac{B_0 B_1}{B_2^2}\right)^2 \left[\frac{\mathrm{cov}(B_0, B_1)}{B_0 B_1} - \frac{\mathrm{cov}(B_0, B_2)}{B_0 B_2} - \frac{\mathrm{cov}(B_1 B_2)}{B_1 B_2} + \frac{\mathrm{var}(B_2)}{B_2^2} \right] \quad \ldots (56)$$

and the covariance matrix D_{B/B_2} of the B_i/B_2 terms is given by

$$D_{B/B_2} = \begin{bmatrix} \mathrm{var}\left(B_0/B_2\right) & \mathrm{cov}\left(B_0/B_2, B_1/B_2\right) \\ \mathrm{cov}\left(B_0/B_2, B_1/B_2\right) & \mathrm{var}\left(B_1/B_2\right) \end{bmatrix} \quad \ldots (57)$$

This latter expression is used to determine the perturbation terms on of the eigenvalues of matrix $\mathbf{A_B}$. Solving the eigenvalues of the matrix $\mathbf{A_B}$ given by Equation (13), the eigensolution for the kth eigenvalue becomes

$$\left(\mathbf{A_B} - \mu_{Vk} I\right) \underline{x}_{VR_k} = 0 \quad \text{or} \quad \left(A_B^T - \mu_{Vk} I\right) \underline{x}_{VL_k}^T = 0 \quad \ldots (58)$$

where $\underline{X}_{VR_k}$ and $\underline{X}_{VL_k}$ are the right and left eigenvectors (a column vector) of the corresponding eigenvalue, respectively.

The eigensolution of the matrix $\mathbf{A_B}$ for the kth eigenvalue (Equation (58)) perturbed with $N_B = \Delta_B \eta_B$ (where η_B is scalar and $\|\Delta_B\|_2 = 1$) takes the form

$$\left(\mathbf{A_B} + \Delta_B \eta_B\right) \underline{x}_{VR_k}\left(\eta_B\right) = \mu_{Vk}\left(\eta_B\right) \underline{x}_{VR_k}\left(\eta_B\right) \quad \ldots (59)$$

Where $\underline{X}_{VR_k}$ and μ_{Vk} are differentiable functions of η_B around the origin such that $\mu_{Vk}(0) = \mu_{Vk}$ and $\underline{X}_{VR_k}(0) = \underline{X}_{VR_k}$. Differentiating Equation (59) with respect to η_B in a similar way to that in Section 3.1 and then pre-multiplying both with $\underline{x}_{VL_k}^H$ leads to

$$\mathrm{d}\mu_{Vk} = \frac{\underline{x}_{VL_k}^H \Delta_B \underline{x}_{VR_k}}{\underline{x}_{VL_k}^H \underline{x}_{VR_k}} \quad \ldots (60)$$

If perturbation on each element of the matrix $\mathbf{A_B}$ is represented by the term $\eta_{B_{pq}}$ of the matrix $\mathbf{N_B}$ (same order as the matrix $\mathbf{A_B}$) given by

$$\mathbf{N_B} = \begin{bmatrix} 0 & \eta_{B_{1,2}} \\ 0 & \eta_{B_{2,2}} \end{bmatrix} \quad \ldots (61)$$

Then the resulting perturbation terms in the kth eigenvalue μ_{Vk} through the application of chain rule and Maclaurin Series expansions (as can be seen in Section 3.1) takes the form

$$\mu_{Vk}\left(\eta_B\right) = \mu_{Vk_0} + \mathrm{d}\mu_{Vk}\left(\eta_B\right) = \mu_{Vk_0} + \underline{J}_{\mu V_k}^T \underline{\eta}_B \quad \ldots (62)$$

where $\underline{J}_{\mu V_k}^T = \sum_{pq} \frac{x_{VL_{k,p}}^H x_{VR_{q,k}}}{\underline{x}_{VL_k}^H \underline{x}_{VR_k}}$ includes the perturbation terms corresponding to μ_{Vk} and $x_{VL_{k,p}}$ is the pth element of the kth left eigenvector, $x_{VR_{q,k}}$ is the qth element of the kth right eigenvector such that the subscripts p and q represent every second term of the vectors with the vector of perturbation terms $\underline{\mathrm{h}}_B$ also comprising the second terms in each row of the perturbation matrix $\mathbf{N_B}$. Hence, the vector of the kth eigenvalue perturbation terms $\underline{J}_{\mathrm{m}V_k}$ is of the order 1×2 and combining the above expression in a matrix form gives

$$\underline{\mu}_V - \underline{\mu}_{V_0} = J_{\mu_V} \underline{\eta}_B \quad \text{and} \quad \left(\underline{\mu}_V - \underline{\mu}_{V_0}\right)^T = \underline{\eta}_B^T J_{\mu_V}^T \quad \ldots (63)$$

where $\mathbf{J_{\mu V}}$ is the matrix of perturbation terms of the corresponding eigenvalues.

The variance of the eigenvalues σ_v^2 can then be found as the diagonal terms of the covariance matrix $\mathbf{D_v}$ such that

$$\mathbf{D_V} = E\left(J_{\mu_V} \underline{\eta}_B \underline{\eta}_B^T J_{\mu_V}^T\right) = J_{\mu_V} E\left(\underline{\eta}_B \underline{\eta}_B^T\right) J_{\mu_V}^T = J_{\mu_V} D_{B/B_2} J_{\mu_V}^T \quad \ldots (64)$$

The diagonal terms of the matrix in Equation (64) represent the variances on the eigenvalues. The lowest positive eigenvalue is the required flutter speed, hence, the corresponding diagonal value representing the variance on the predicted flutter speed $\sigma_{V_F}^2$ can be used to determine the 95% confidence bound on the flutter prediction.

4.0 RESULTS

The statistical technique described above was applied on data from two different simulated aeroelastic models. Initially a binary flutter system was used to evaluate the method and then a full scale four-engined passenger aircraft (SIM2 Model) was investigated.

4.1 Simulation setup

Zero noise frequency and damping ratio trends for both systems against airspeed, calculated from the eigensolution, are shown in Figs 1 and 2. Only the lowest frequencies are shown for the SIM2 model results. For the binary flutter system the flutter speed for the chosen structural parameters was found to be 46ms^{-1}, while for the SIM2 model, flutter occurred at 188·38ms^{-1}.

https://doi.org/10.1017/S0001924000002761 Published online by Cambridge University Press

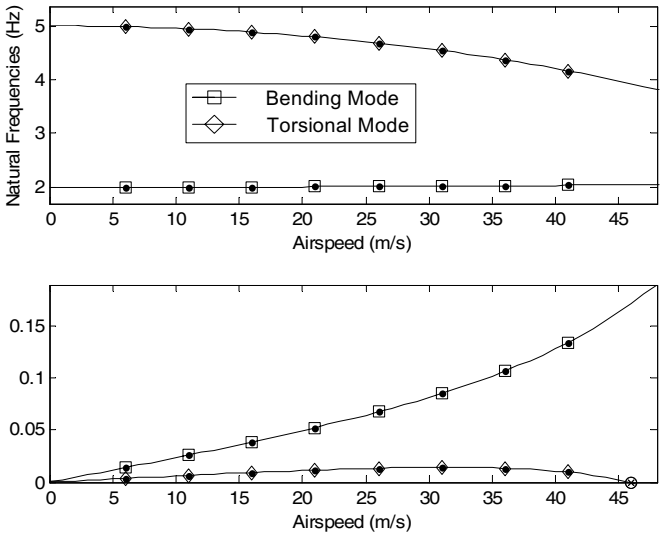


Figure 1. Frequency and damping trends (binary system).

Chirp signal excitation was applied covering the desired system bandwidth and the response determined via numerical integration of the aeroelastic equations. The decay response data for the binary flutter system and the SIM2 model were recorded at a sampling rate of 0·04s and 0·01s, respectively. Impulse response functions were then generated for application of the LSCE method using overspecified estimates. For the binary system, the simulations were run at 5ms^{-1} airspeed increments whilst those for the SIM2 model were run with increments of 15ms^{-1}. Different speed ranges between 50% and 90% of the respective true flutter speeds were taken keeping in view the fact that the flutter margin approach is more effective closer to the actual flutter boundary[11]. In each case, the flutter speed was predicted using the flutter margins along with 95% confidence bounds on the predicted flutter speed. Different measurement noise levels were considered.

4.2 Binary aeroelastic system

Table 1 shows the flutter speed predictions obtained using the two statistical approaches applied to a single data set at each flight test point and also Monte-Carlo simulations for flutter margin and flutter speed predictions. Figures 3 show typical plots of the flutter margin confidence envelopes. The bounds obtained by the statistical approach are affected by increases in the noise corruption.

The statistical curvefitting approach gave very comparable bounds of the flutter speed compared to the Monte-Carlo simulations. The full statistical approach also gave reasonable flutter speed bounds compared with the Monte-Carlo simulations at low noise levels; however there was a significant degradation in the results once the noise level increased.

4.3 SIM2 Model

Table 2 shows the flutter speed predictions with confidence bounds for the SIM2 model. The statistical curvefitting and full statistical approaches gave comparable bounds for low levels of measurement noise. However, the comparison of the statistical approaches with the Monte-Carlo simulations is not good. One major problem that was encountered was the use of the LSCE identification method meant that a large amount of model overspecification was required in order to achieve unbiased estimates of the modes of interest, and this resulted in ill-conditioning problems with the calculation of the statistical bounds.

5.0 DISCUSSION AND CONCLUSIONS

An approach has been introduced that determines the statistical confidence bounds on flutter speed predictions using the flutter margin method based upon a single set of test data. The method is based upon least squares statistics and eigenvalue perturbation theory at different phases of the process without the need for Monte-Carlo analysis of repeated tests or individual test sequences. The approach was applied to simulated flight flutter data from two different aeroelastic systems and comparison was made with flutter speed estimates from Monte-Carlo simulations.

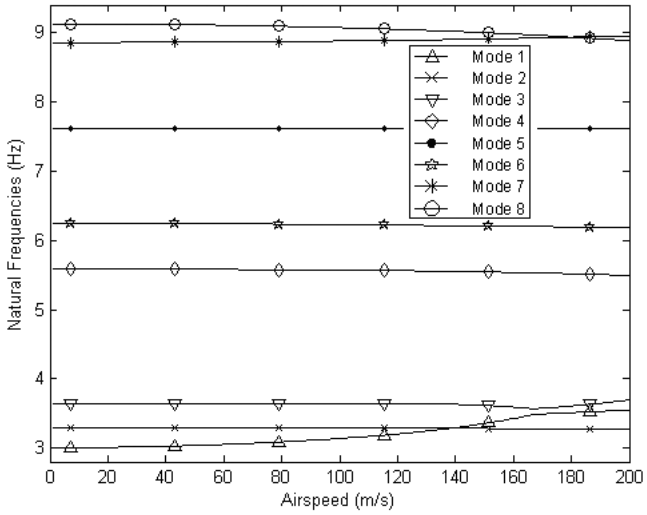


Figure 2(a). Frequency trends (SIM2).

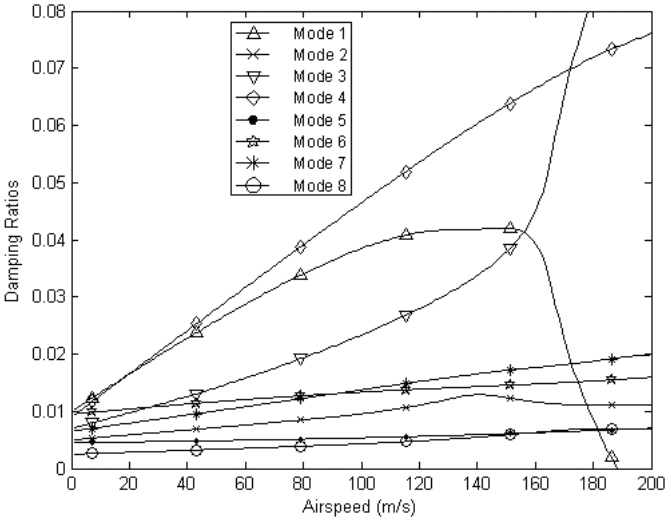


Figure 2(b). Damping trends (SIM2).

https://doi.org/10.1017/S0001924000002761 Published online by Cambridge University Press

Table 1
Binary aeroelastic system — flutter speed predictions

	True flutter speed 46ms^{-1}								
Test speeds (% of true flutter speed)	50% to 82%			60% to 90%			50% to 90%		
Measurement noise (%)	1	5	10	1	5	10	1	5	10
Statistical analysis (1 simulation data set)									
Predicted flutter speed (VF -ms^{-1})	43·91	44·95	48·89	43·31	44·04	51·12	43·10	44·80	48·72
Error in VF (%)	–4·53	–2·29	6·27	-5·84	–4·25	11·14	–6·31	-2·61	5·92
±95% confidence bound on VF (curvefit approach– ms^{-1})	5·22e–3	1·77e–2	1·09e–1	5·67e–4	1·01e–2	9·55e–2	8·00e–4	5·83e–3	7·56e–2
±95% confidence bound on VF (statistical approach– ms^{-1})	9·10e–2	1·94e+3	1·37e+4	9.29e–2	3·69e+3	1·04e+4	7·32e–2	1·21e+3	6.47e+3
Monte Carlo analysis (100 simulations)									
Predicted flutter speed (VF - ms^{-1})	43·43	46·05	47·22	44·27	46·41	46·01	44·00	46·25	46·19
Error in VF (%)	–5·58	0·12	2·65	–3·75	0·89	0·02	–4·34	0·54	0·42
±95% confidence bound on VF (ms^{-1})	9·93e–3	6·47e–2	1·04e–1	8·97e–3	4·43e–2	5·22e–2	7·11e–3	3·15e–2	5·86e–2

Table 2
SIM2 Model — Flutter speed predictions

	True flutter speed 188·38ms^{-1}								
Test speeds (% of true VF)	50% to 82%			60% to 90%			50% to 90%		
Measurement noise (%)	1	5	10	1	5	10	1	5	10
Statistical analysis (1 simulation data set)									
Predicted flutter speed (VF – ms^{-1})	193·48	183·29	177·36	192·50	180·78	180·28	193·73	180·27	178·57
Error in VF (%)	2·70	–2·70	–5·85	2·18	–4·04	-4.30	2.84	–4·31	–5·21
±95% Confidence bound on VF (curvefit approach– ms^{-1})	5·09e–5	1·34e–4	2·52e–4	3·76e–5	6·22e–5	1·41e–4	1·31e–4	1·87e–4	2·78e–4
±95% Confidence bound on VF (statistical approach– ms^{-1})	6·55e–4	1·92e–3	4·25e–3	1·58e+0	7·70e+0	7·83e+1	1·25e-3	1·90e-3	2·57e+1
Monte Carlo analysis (100 simulations)									
Predicted flutter speed (VF - ms^{-1})	227·23	176·81	174·71	192·31	181·49	180·73	198·36	179·96	179·47
Error in VF (%)	20·62	–6·14	–7·26	2·08	–3·66	–4·06	5·29	–4·47	–4·73
±95% confidence bound on VF (ms^{-1})	9·24e–1	1·22e–1	2·25e–1	7·47e–2	7·52e–2	1·73e–1	1·19e–1	6·22e–2	2·07e–1

Results on the simple binary flutter system were encouraging, particularly the simpler curve-fitting approach, and good comparison was achieved compared to the Monte-Carlo simulations. The results on the more realistic aeroelastic model were less convincing, and there are questions that can be raised about the robustness of the approach when applied to noisy data. This weakness is probably due to the number of approximations (e.g. assuming first term in series expansions and statistics of the noise) that are made throughout the chain of calculations required to obtain the confidence bounds on the flutter speeds, and also the issue of overspecification of the identification model. The use of model order overspecification for the identification process reduces the scatter of estimated modes of interest and arguably comparison with the Monte-Carlo simulation results should not lead to exactly the same confidence bounds; the statistical approach bounds are less than those from the simulations. Further investigation is required to make the procedure more robust, for instance by using a minimum order realisation identification method such as ERA or ERA/DC which would alleviate spurious mode problems.

ACKNOWLEDGEMENTS

The first author would like to acknowledge the support of the National Centre for Physics, Islamabad, Pakistan.

https://doi.org/10.1017/S0001924000002761 Published online by Cambridge University Press

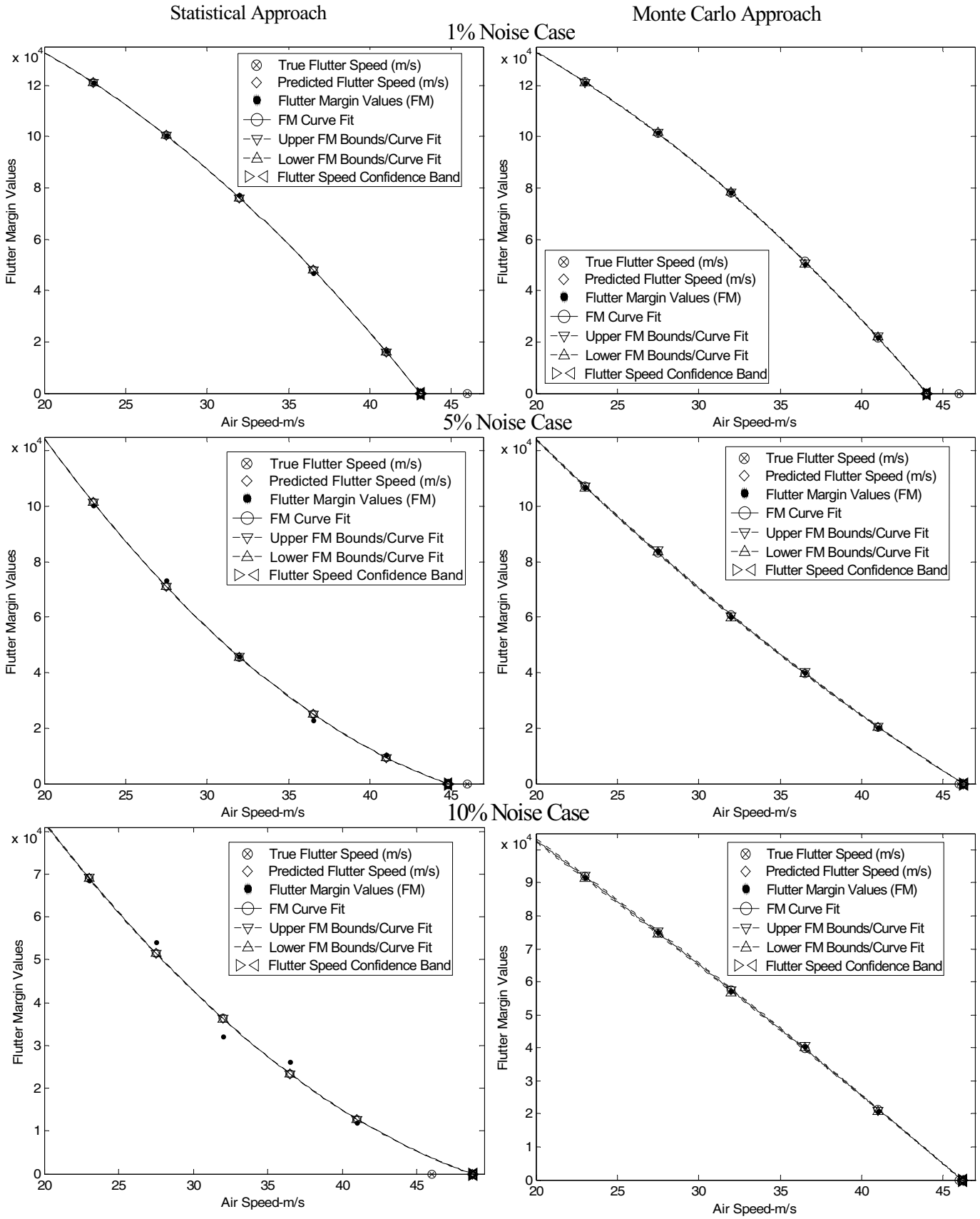


Figure 3. Flutter margin bounds for binary system under different noise levels.
Left hand column — statistical approach, Right hand column – Monte Carlo simulation.

https://doi.org/10.1017/S0001924000002761 Published online by Cambridge University Press

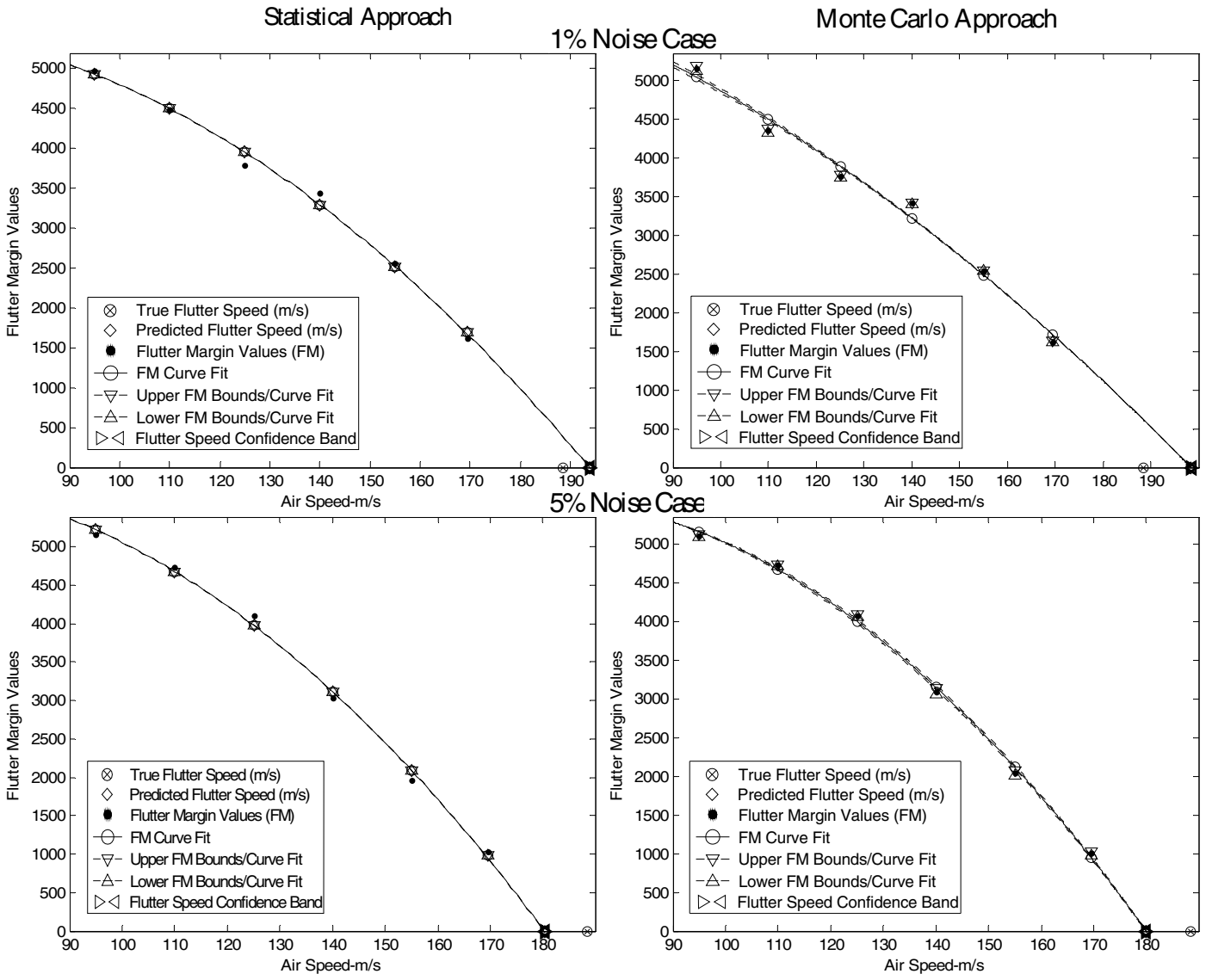


Figure 4. Flutter margin bounds for different noise levels (SIM2 Model).
Left hand column = statistical approach, right hand column = Monte Carlo simulation.

REFERENCES

1. GARRICK, I.E. and REED, W.H. Historical development of aircraft flutter. *J Aircr*, 1981, **18**, (11), pp 897-912.
2. WRIGHT, J.R. and COOPER, J.E. *Introduction to Aircraft Aeroelasticity and Loads*, 2007, John Wiley & Sons.
3. COLLAR, A.R. The first fifty years of aeroelasticity, *Aerospace*, February 1978, **545**, pp 12-20.
4. KEHOE, M.W. A historical overview of flight flutter testing, AGARD Conference Proceedings 566, 1995, Advanced Aeroservoelastic Testing and Data Analysis, Rotterdam, The Netherlands.
5. COOPER, J.E. *ET AL*. Advances in the analysis of flight flutter test data, Advanced Aeroservoelastic Testing and Data Analysis (CP-566), 1995, Rotterdam.
6. ZIMMERMAN, N.H. and WEISSENBERGER, J.T. Prediction of flutter onset speed based on flight flutter testing at subcritical speeds, *J Aircr*, 1964. **1**, (4), pp 190-202.
7. NISSIM, E. and GILYARD, G.B. Method for experimental determination of flutter speed by parameter identification, 1989, AIAA-89_1324-CP.
8. COOPER, J.E., DESFORGES, M.J. and WRIGHT, J.R. The on-line envelope function — a guide to aeroelastic stability, 1993, IFASD Conference, pp 981-997.
9. COOPER, J.E., EMMETT, P.R. and WRIGHT, J.R. Envelope function — a tool for analyzing flutter data, *J Aircr*, 1993, **30**, (3), pp 785-790.
10. TORII, H. and MATSUZAKI, Y. Flutter margin evaluation for discrete-time systems, *J Aircr*, 2001, **38**, (1), pp 42-47.
11. DIMITRIADIS, G. and COOPER, J.E. Flutter prediction from flight flutter test data, *J Aircr*, 2001, 38, (2), pp 355-367.
12. LIND, R. Flight test evaluation of flutter prediction methods, *J Aircr*, 2003, 40, (5), pp 964-970.
13. LIND, R.C. Flight testing with the flutterometer, *J Aircr*, 2003, **40**, (3), pp 574-579.
14. LIND, R.C. and BRENNER, M. The flutterometer: an on-line tool to predict robust flutter margins, *J Aircr*, 2000, **37**, (6), pp 1105-1112.
15. LIND, R.C. Robust flutter margin analysis that incorporates flight data, 1998, NASA/TP-1998 206543.
16. LIND, R.C. and BRENNER, M. Robust flutter margins of an F/A-18 aircraft from aeroelastic flight data, *J Guidance, Control and Dynamics*, 1997, **20**, (3), pp 597-604.
17. PETIT, C.L. Uncertainty quantification in aeroelasticity: recent results and research challenges, *J Aircr*, 2004, **41**, (5), pp 1217-1229.
18. PETERSON, L.D., S.J. BULLOCK and S.W. DOEBLING, The statistical sensitivity of experimental modal frequencies and damping ratios to measurement noise, *Modal Analysis (USA)*, 1996, **11**, (1), pp 63-75.

https://doi.org/10.1017/S0001924000002761 Published online by Cambridge University Press

19. BERGMANN, M., LONGMAN, R.W. and J.-N. JUANG. Variance and bias computation for enhanced system identification, 1989, 28th IEEE Conference on Decision and Control.
20. PERRIOT, A., RAYNAUD, J.L. and S. COGAN. Uncertainties in identified modal parameters, 1998, ISMA23.
21. DOEBLING, S.W. and FARRAR, C.R. Estimation of statistical distributions for modal parameters identified from averaged frequency response function data, *J Vibration and Control*, 2001, **7**, (4), pp 603-624.
22. FARRAR, C.R., DOEBLING, S.W. and CORNWELL, P.J. A comparison study of modal parameter confidence intervals computed using the Monte Carlo and Bootstrap techniques, 1998, 16th International Modal Analysis Conference, Santa Barbara, California, pp 936-944.
23. LONGMAN, R.W. *ET AL*. Variance and bias computation for improved modal identification using ERA/DC, 1991, American Control Conference, Boston, MA.
24. TROYER, T.D. *ET AL* Fast derivation of uncertainty bounds for on-line flight flutter testing, 2006, ISMA, Leuven, Belgium.
25. PINTELON, R., GUILLAUME, P. and SCHOUKENS, J. Uncertainty calculation in (operational) modal analysis, *Mechanical Systems and Signal Processing*, 2007, **21**, (6), pp 2359-2373.
26. GUILLAUME, P., VERBOVEN, P. and VANLANDUIT, S. Frequency-domain maximum likelihood identification of modal parameters with confidence intervals. 1998, ISMA 23.
27. POIREL, D., DUNN, S. and PORTER, J. Flutter-margin method accounting for modal parameter uncertainties, *J Aircr*, 2005, 42, (5), pp 1236-1243.
28. PRICE, S.J. and LEE, B.H.K. Evaluation and extension of flutter-margin method for flight flutter prediction, *J Aircr*, 1993, **30**, (3), pp 395-402.
29. HEEG, J. Stochastic characterization of flutter using historical wind tunnel data, 2007, 48th AIAA SDM Conference.
30. COOPER, J.E. Comparison of some time domain system identification techniques using approximate data correlations, I*nt J Analytical and Experimental Modal Analysis*, 1989, **4**, (2), pp 51-57.
31. BROWN, D.L. *ET AL* Parameter estimation techniques for modal analysis, 1979, SAE Technical Paper 790221.
32. DEBLAUWE, F., BROWN, D.L. and ALLEMANG, R.J. The polyreference time domain technique, 1987, IMAC V, pp 832-845.
33. JUANG, J.N. and PAPPA, R.S. An eigensystem realization algorithm for modal parameter identification and model reduction, *J Guidance, Control and Dynamics*, 1985. **8**, (5), pp 620-627.
34. OVERSCHEE, P.V. and MOOR, B.L.D. *Subspace Identification for Linear Systems: Theory, Implementation, Applications*, 1996, p 256, Kluwer Academic Publishers.
35. BENINI, G.R. *ET AL* Flutter clearance of a non-linear aircraft, 2005, International Forum on Aeroelasticity and Structural Dynamics, Munich, Germany.
36. KATZ, H., FOPPE, F.G. and GROSSMAN, D.T. F-15 Flight Flutter Test Program, 1976, NASA SP-415, pp 413-431, NASA, Washington, DC.
37. COOPER, J.E., EMMETT, P.R. and WRIGHT, J.R. A statistical confidence factor for modal parameter identification, 1992, 17th International Seminar on Modal Analysis, pp 1611-1626.
38. DIMITRIADIS, G. and COOPER, J.E. Online flight flutter testing, 2001, International Conference on Structural System Identification, Kassel, Germany.
39. DESFORGES, M.J., COOPER, J.E. and WRIGHT, J.R. Spectral and modal parameter estimation from output-only measurements, *Mech Systems and Signal Processing*, 1995, **9**, (2), pp 169-186.
40. MUCHERONI, M.F. and CARDOSO, A. Output-only structural identification of random vibrating systems, *J Brazilian Society of Mechanical Sciences and Engineering*, 2006, **28**, (1), pp 99-104.
41. LONGMAN, R.W. and JUANG, J.-N. A variance based confidence criterion for ERA identified modal parameters, AAS/AIAA Astrodynamics Specialist Conference, 1987, Kalispell, Montana.
42. MARKOVSKY, I. *ET AL* When is a pole spurious? 2006, International Conference on Noise and Vibration Engineering (ISMA 2006).
43. GUILLAUME, P., SCHOUKENS, J. and PINTELON, R. Sensitivity of roots to errors in the coefficients of polynomials obtained by frequency-domain estimation methods, IEEE transactions on instrumentation and measurement, 1989, **38**, (6), pp 1050-1056.
44. GOLUB, G.H. and LOAN, C.F.V. *Matrix Computations*, 2nd Edition, 1996, Baltimore, London: Johns Hopkins University Press.
45. KENDALL, M.G., A. STUART, and J.K. ORD, *The Advanced Theory of Statistics*, 4th Edition, Design and Analysis, and Time-Series Vol 3, 1983, Charles Griffin & Company, London.
46. YATES, F. *Sampling Methods for Censuses and Surveys*. 4th Edition, 1981 Charles Griffin & Company, London.
47. DIETERS, M.J. ET AL. Application of approximate variances of variance components and their ratios in genetic tests, *Theoretical and Applied Genetics*, 1995, **91**, (1), pp 15-24.
48. BLUMENFELD, D. *Operations Research Calculations Handbook*, 2001, Boca Raton, FL 33431, CRC Press.
49. FUNKHOUSER, E.M. and M. GROSSMAN, Bias in estimation of the sampling variance of an estimate of heritability. *J Heredity*, 1982, **73**, (2), pp 139-141.
50. PEARSON, K. Mathematical contributions to the theory of evolution.—on a form of spurious correlation which may arise when indices are used in the measurement of organs, Royal Society of London, 1897, **60**, (1896-1897), pp 489-498.

https://doi.org/10.1017/S0001924000002761 Published online by Cambridge University Press